THE EFFECT OF POROSITY ON INFRARED SPECTRA. J. A. Arnold[1], R. Schräpler[2], K. L. Donaldson Hanna[1], S. S. Lindsay[1,3], N. E. Bowles[1] and J. Blum[2] [1]University of Oxford (jessica.arnold@physics.ox.ac.uk), [2]Technische Universität Braunschweig, [3]University of Tennessee

Introduction: The low gravitational acceleration on asteroids, the Moon, and other small, airless solar system bodies allows for the formation of high porosity regolith [1,2]. These conditions, in particular the gravity environment, are not easily replicated in a laboratory setting.

Laboratory studies of regolith analogues show that sample loading technique has a significant impact on both emissivity and reflectance spectra. For lunar soils and analogues, sample compaction results in changes to both the overall spectral slope and the transparent regions of the spectra [3,4,5]. Across visible and near-infrared (VNIR) wavelengths, compacted powder has higher overall reflectance compared with loose powder [6]. It is unclear as of yet if these spectral changes are due to differences in porosity at the very top (10's of μm) of the sample, subtle changes in submillimeter-scale surface topography, or a combination of these two factors. However, porosity by itself is likely important as evidenced by the reproducibility of emission features observed in certain asteroid (e.g. Trojan) spectra with suspensions of mineral or meteorite powder in a KBr powder matrix [7]. Here, we present emissivity and reflectance measurements of samples with well-characterized porosity vs. depth profiles, as well as numerical models of high porosity regolith emissivity spectra.

Samples and Methods: In this initial study, we used two sets of mono-disperse smooth, spherical SiO_2 particles with diameters of 1.5 μm and 10 μm (manufacturer: micromod Partikeltechnologie GmbH). This material is useful as both an analog to silicate regolith and a test of our radiative transfer model. The 1.5 μm particle sample was prepared using the setup described in [8]. Briefly, SiO_2 is loaded into cylindrical containers within a revolver mechanism. Each parcel of dust is pushed onto a rotating cogwheel whose purpose is to de-agglomerate the sample into single grains. Ambient gas at roughly 100 Pa flows through the vacuum chamber to allow each grain to be deposited on a thin filter substrate. After running this setup for a few hours, a roughly cylindrical dust sample of 25 mm in diameter and a few mm thick is produced. To collect spectra, we slide the sample with the filter substrate into a sample cup. The 10 μm particle sample was prepared by shaking the sample container and then leaving it to settle through gas diffusion for at least 1 hour. Visible–near infrared (VNIR) and mid infrared (MIR) diffuse reflectance and thermal infrared (TIR) emissivity measurements were collected for both of these samples using facilities within the Planetary Spectroscopy Facility at the University of Oxford. For the 1.5 μm sample, we also measured VNIR and MIR diffuse reflectance of two different compacted surfaces and a broken surface. The porosity with depth for the freshly prepared surfaces was estimated from x-ray tomography (XRT) of identically prepared samples (Fig 1). The packing fraction of the compacted surfaces (ϕ=0.45, ϕ=0.50) were estimated from the known density of the silica spheres and the volume of the sample well.

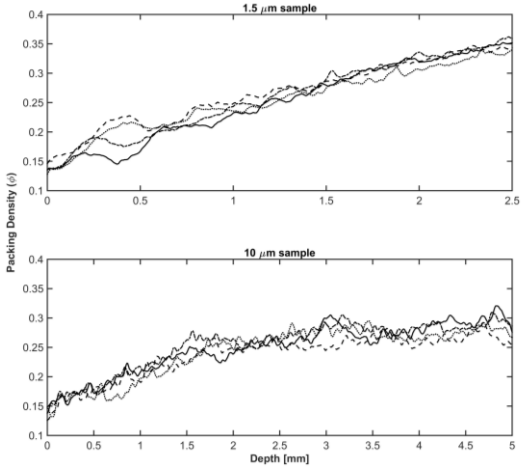

Figure 1: Packing density profiles of four spots on each surface estimated from XRT, averaged over a disc of 1mm diameter from top of sample parallel to the cylindrical axis.

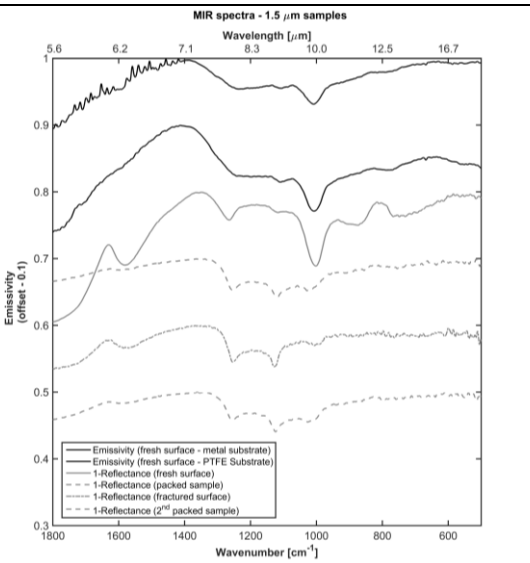

Figure 2: Emissivity and diffuse reflectance measurements of silica, with offset of 0.1 for clarity. Diffuse reflectance is presented as ε = 1-R for comparison with emissivity measurements.

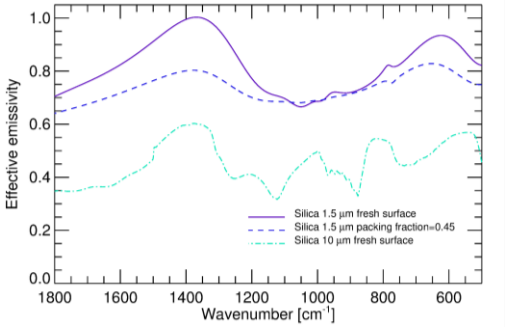

Figure 3: Modeled emissivity spectra of silica, offset 0.2 for clarity.

Thermal transfer model and porosity corrections: We started with a currently existing, layered, plane-parallel radiative transfer model [9]. This model couples Mie scattering with the DISORT radiative transfer code to calculate near-surface thermal gradients for a layered regolith as a function of various environmental conditions. However, as [10] demonstrates, the single scattering albedo and asymmetry parameters derived from Mie theory are not suitable for densely packed media. A few different approaches been developed to deal with this issue. To test these various methods, we have built a choice of packing corrections into the code from [9], briefly outlined below, which were applied to quartz optical constants from [11]. To model silica, we derived optical constants from reflectance spectra of mounted and polished 250 µm spheres.

Diffraction subtraction. For close-packed, large particles, [12] assumes that the diffraction components of the single scattering albedo and asymmetry parameter can be removed.

Static structure factor. One way to deal with close-packing is to modify the scattering phase function, which in turn affects the single scattering and asymmetry parameters. The static structure factor is a statistical mechanics-based correlation function for spheres in a fluid medium. We use the formulation from [10], which shows that an approximate form of this function [13] produces more realistic asymmetry parameter values.

Effective medium theory. There are various mixing relations used to obtain effective indices of refraction for Mie scattering calculations [14]. We looked at two of these: 1) the Maxwell-Garnett mixing rule, which assumes small (Rayleigh-scale) inclusions within a matrix and 2) the Bruggeman mixing rule, which applies to an intimate mixture of two materials, one of which can be air or vacuum. The applicability of these mixing rules to wavelength-sized particles has not been tested in either laboratory measurements or modeling studies.

Results: Silica is transparent in the VNIR, showing only absorptions due to H_2O (1.35 µm, 1.9 µm, 2.7-3 µm) and Si-OH (2.2 µm, 2.6 µm). In the MIR, there is good agreement between the diffuse reflectance and emissivity measurements of the fresh, uncompacted samples for both particle sizes. The reflectance feature in the diffuse spectra at ~1250 cm^{-1} is dependent on the incidence angle [15]. The MIR diffuse reflectance and emissivity spectra of the 1.5 µm sample (Fig 2) show changes in the shape of the Christiansen feature (an emissivity maximum near 1400 cm^{-1}, or 7 µm) with porosity. Note that this feature may be affected by the geometry of the biconical diffuse reflectance setup, which can cause mis-identification of the CF [16]. Moreover, the spectral contrast of the 1000 cm^{-1} (10 µm) feature is reduced in both the packed and broken surfaces. The similarity of the broken surface to the packed surfaces is likely because, although the sample may remain porous at depth, the top few layers of a disturbed sample will have a high packing fraction.

Of the porosity corrections tested, the static structure factor best replicated changes in band depth while preserving band shape. To model the fresh, uncompacted samples of each particle size, we applied the static structure factor using the respective packing density profiles shown in Fig 1. We also modeled the 1.5 µm packed sample with a constant packing density of ϕ=0.45. Modeled spectra are shown in Fig 3. First, focusing on the 1.5 µm samples, the more porous sample has a steeper spectral slope short-ward of the Christiansen feature and a narrow 1000 cm^{-1} feature, in agreement with measurements. However, the spectral contrast of the 1000 cm^{-1} feature is underestimated, while the depth of the feature at 875 cm^{-1} (11.45 µm) is over-estimated. Next, looking at the difference between the particle sizes, the model shows a 700 cm^{-1} (14.2 µm) feature that is present in the 10 µm sample, but not the 1.5 µm samples, in agreement with measured spectra.

References: [1] Hapke B. (1993) *Theory of Reflectance and Emittance Spectroscopy*, p. 224. [2] Carrier W.D. et al. (1991) In *Lunar Sourcebook* (Heiken G.H., Vaniman D.T., and French B.M., Eds.), pp. 475–594. [3] Logan L.M. et al. (1973) *JGR, 78*, 23, 4983–5003. [4] Salisbury J.W. and Eastes J.W. (1985) *Icarus, 64*, 586-588. [5] Donaldson Hanna K.L. et al. (2014) *ELS*, p. 91. [6] Shepard M.K. and Helfenstein P. (2011) *Icarus, 215*, 2, 526–533. [7] Vernazza P. et al. (2012) *Icarus, 221*, 2, 1162–1172. [8] Blum J. et al. (2006) *Astrophys. J., 652*, 1768–1781. [9] Milan L. et al. (2011) *JGR, 116*, E12003. [10] Mishchenko M.I. (1994) *J. Quant. Spec., 52*, 1, 95–110. [11] Spitzer W.G. and Kleinman D.A. (1961) *Phys. Rev. 121*, 1324. [12] Wald A.E. (1994) *JGR, 99*, B12, 24241–24250. [13] Wertheim M.S. (1963) *PRL, 10*, 8, 321–322. [14] Voshchinnikov N.V. et al. (2007) *Appl. Opt., 46*, 19, 4065–4072. [15] Almeida R.M. (1992) *Phys. Rev. B 45*, 161.Salisbury J.W. and D'Aria D. (1989) *LPS XX*, p. 941.